**A UNIFIED MODEL FOR
LONGITUDINAL AND LATERAL WEB
DYNAMICS**

Jerry Brown
NormalEntry.com

INTRODUCTION

In "The Effect of Mass Transfer on Multi-Span Lateral Dynamics of Uniform Webs" [1], it is shown that behavior of Shelton's lateral dynamic beam model [2] can be explained as the interaction of the normal entry equation and mass transfer between spans. The implications of mass transfer are discussed further in "The Connection Between Longitudinal and lateral Web Dynamics" [3]

In this paper, the mass transfer idea is generalized and used to develop a dynamic model that combines lateral and longitudinal (tension) behavior. Nonlinear elasticity theory is used to model the web as a two-dimensional membrane in a state of plane stress. Boundary conditions at the downstream roller are: 1) the normal entry equation, used in lateral models, and 2) the continuity equation, used in tension models.

Results from the new model, such as lateral force, lateral position, face angle and slope are shown to agree closely with the static and dynamic beam models developed and tested by Shelton [2]. Comparisons are also made with the dynamic beam model from reference [1] that includes the effect of shear.

Information that is unique to the two-dimensional model is presented and discussed, such as,

1. Transient disturbances in tension at the downstream roller caused by pivoting and shifting of rollers.
2. Transient gradients in lateral velocity that can cause wrinkling.
3. The effect of tension change on lateral position.

NOMENCLATURE

A cross sectional area of web
d_{shift} lateral shift of roller
E elastic modulus
G shear modulus
h thickness of web
I area moment of inertia

L	span length
Q	mass flow rate
t	time
T	tension in units of force
u	x displacement of deformed web
v	y displacement of deformed web
V_o	web velocity in machine direction
x	distance along length of web
y	lateral displacement of web
y_0	lateral web displacement at upstream roller, relative to ground
y_L	lateral web displacement at downstream roller, relative to ground
z	lateral displacement of roller relative to ground
β	boundary defect angle
η	y coordinate of deformed web
ε_{xx}	strain in x direction
ε_{yy}	strain in y direction
ε_{zz}	strain in z direction
θ_r	angle of roller axis
γ_{xy}	shear strain
μ	Poisson's ratio
ϕ	face angle, rotation of cross section or bending angle
ρ	density
σ_{xx}	stress in x direction
σ_{yy}	stress in y direction
σ_{zz}	stress in z direction
τ_{xy}	shear stress in x-y plane
ξ	x coordinate of deformed web
ψ	shear angle
ω_z	rotation in x-y plane
$_0$	subscript indicating value of variable at $x = 0$
$_L$	subscript indicating value of variable at $x = L$

A 2-DIMENSIONAL MODEL THAT COMBINES LATERAL AND LONGITUDINAL BEHAVIOR

Plane Stress Definitions

The following equations for plane stress are taken from Novozhilov's simplified nonlinear theory for small rotations [4].

Classical linear elasticity theory assumes that rotations are so small that their effects are negligible. This is not true in web handling problems where longitudinal tension affects the elastic curve. The $\omega_z \sigma_{xx}$ term in equilibrium equation (12) is particularly important. Without it, the effects of longitudinal tension on the elastic curve will not be reflected in the results. Its net effect in web analysis is very similar to the second order derivative term in Shelton's beam theory differential equation for the elastic curve of a web under tension at a misaligned roller [2], (Pg. 58).

Some applications of nonlinear elasticity also require inclusion of the effects of rotation on strains. However, for analysis of a misaligned roller this effect is sufficiently small that the ω_z terms in equations (2) and (3) may be safely ignored.

Although the stresses and strains defined below are identified by subscripts x, y and z, it is understood that these quantities are aligned with the corresponding curvilinear coordinate system of the deformed web.

Displacements in the direction of the reference coordinates x and y are defined as u and v, respectively and,

Rotation in x-y plane
$$\omega_z = \frac{1}{2}\left(\frac{\partial v}{\partial x} - \frac{\partial u}{\partial y}\right) \tag{1}$$

Strain in the x direction
$$\varepsilon_{xx} = \frac{\partial u}{\partial x} + \frac{1}{2}\omega_z^{\,2} \cong \frac{\partial u}{\partial x} \tag{2}$$

Strain in the y direction
$$\varepsilon_{yy} = \frac{\partial v}{\partial y} + \frac{1}{2}\omega_z^{\,2} \cong \frac{\partial v}{\partial y} \tag{3}$$

Shear strain
$$\gamma_{xy} = \frac{\partial u}{\partial y} + \frac{\partial v}{\partial x} \tag{4}$$

Strain in the z direction
$$\varepsilon_{zz} = \frac{-\mu}{1-\mu}(\varepsilon_x + \varepsilon_y) \tag{5}$$

Cartesian coordinates of the deformed web are,

$$\xi = x + u \tag{6} \qquad\qquad\qquad \eta = y + v \tag{7}$$

Assuming Hook's Law, the stresses may be expressed in terms of strains, Poisson's ratio, μ, and modulus of elasticity, E, as follows.

The x-axis stress is:
$$\sigma_{xx} = \frac{E}{1-\mu^2}\left[\varepsilon_{xx} + \mu\varepsilon_{yy}\right] \tag{8}$$

The y-axis stress is:
$$\sigma_{yy} = \frac{E}{1-\mu^2}\left[\varepsilon_{yy} + \mu\varepsilon_{xx}\right] \tag{9}$$

The shear stress is:
$$\tau_{xy} = \frac{E}{2(1+\mu)}\left[\frac{\partial u}{\partial y} + \frac{\partial v}{\partial x}\right] \tag{10}$$

The equations of equilibrium are:

$$\frac{\partial}{\partial x}\left[\sigma_{xx} - \omega_z\tau_{xy}\right] + \frac{\partial}{\partial y}\left[\tau_{xy} - \omega_z\sigma_{yy}\right] = 0 \tag{11}$$

$$\frac{\partial}{\partial y}\left[\sigma_{yy} + \omega_z\tau_{xy}\right] + \frac{\partial}{\partial x}\left[\tau_{xy} + \omega_z\sigma_{xx}\right] = 0 \tag{12}$$

The transformations from undeformed to deformed cartesian coordinates are

$$d\xi = \left(1 + \frac{\partial u}{\partial x}\right)dx + \frac{\partial u}{\partial y}dy \qquad d\eta = \frac{\partial v}{\partial x}dx + \left(1 + \frac{\partial v}{\partial y}\right)dy \tag{13}$$

The equation of continuity

The mass flow rate Q through an increment of cross-sectional area $dy(1+\varepsilon_{yy})h(1+\varepsilon_{zz})$ in a moving web is,

$$Q = V_o\rho\, dy(1+\varepsilon_{yy})h(1+\varepsilon_{zz}) \tag{14}$$

where, ρ is the density of the deformed web, V_o is the local velocity in the direction of the x coordinate, dy is an increment of width in the relaxed web and h is thickness. The thickness h is small enough relative to other dimensions of the web that a condition of plane stress can be

assumed to apply. The density ρ varies with deformation, so it's necessary to make the following conversion.

$$\rho = \frac{\rho_o}{\left(1 + \varepsilon_{xx}\right)\left(1 + \varepsilon_{yy}\right)\left(1 + \varepsilon_{zz}\right)} \tag{15}$$

where ρ_o is the density of the relaxed web.

The mass flow rate Q at any point is, therefore,

$$Q = \frac{V_o}{\left(1 + \varepsilon_{xx}\right)} \rho_o \, h \, dy \tag{16}$$

For purposes of tension analysis, systems are usually modeled as shown in Figure 1. The web is treated as a straight ribbon of constant width w and thickness h. Strains ε_{x1} ε_{x2} and ε_{x3} are assumed to be constant from one roller to the next and driven rollers determine the velocities, V_1 and V_2, at the ends of the span. The length of wrap on the rollers is assumed to be negligible compared to the length of the span and lateral behavior is ignored.
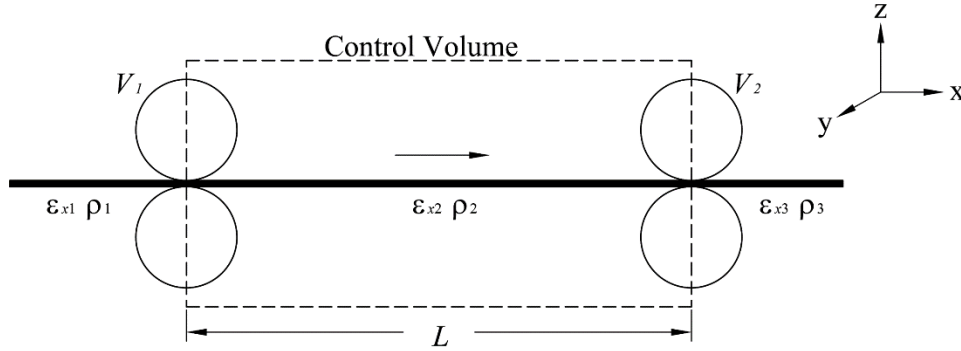

Figure 1
Single span system

The difference in the mass entering and exiting the control volume in a time increment dt must be equal to the change of mass inside it. Therefore,

$$\frac{d}{dt}\int_0^L \frac{1}{1 + \varepsilon_{x2}} \rho_o \, h \, w \, dx = \frac{V_1}{1 + \varepsilon_{x1}} \rho_o \, h \, w - \frac{V_2}{1 + \varepsilon_{x2}} \rho_o \, h \, w \tag{17}$$

Under those assumptions, canceling common factors and using the small strain approximation $1/(1 + \varepsilon) = (1 - \varepsilon)$, equation (17) becomes,

$$\frac{d}{dt}\int_0^L (1 - \varepsilon_{x2}) dx = \frac{d}{dt}\left(-\varepsilon_{x2}L\right) = V_1\left(1 - \varepsilon_{x1}\right) - V_2\left(1 - \varepsilon_{x2}\right) \tag{18}$$

Equation (18) appears as the governing equation in many of the papers on tension control [5, 6].

For a 2D elasticity model, incorporating lateral bending, it is necessary to go back to equation (17) and think about what to do about the integral on the left side when ε_{x2} is a function of x, y. Fortunately, the features of plane stress elasticity theory provide an easy answer.

Looking again at equation (18), the $-\varepsilon_{x2}L$ term is equal to the amount by which the mass of the span differs from what it was when it was relaxed. However, it is also the amount by which the

longitudinal stress causes the length of the web to differ from the length of the control volume. Therefore, in the context of plane strain elasticity theory, $\varepsilon_{x2}L$ is simply the x-direction displacement u at $x = L$, which is found by solving the equations of equilibrium (11) and (12). This suggests that it might be possible to express the continuity equation as equation (20) and use it as a boundary condition. In fact, if ε_{x2} is replaced with expression (2) from elasticity theory, the result is,

$$\int_0^L \left(1 - \frac{\partial u}{\partial x}\right) dx = -u_L \tag{19}$$

and the continuity equation for a narrow strip of width dy becomes,

$$\frac{d}{dt}\left(-u_L\right) = V_1\left(1 - \varepsilon_{x0}\right) - V_2\left(1 - \varepsilon_{xL}\right) \tag{20}$$

where u_L is the x-direction displacement at $x = L$ *due to mass flow* while ε_{x0} and ε_{xL} are the x-direction strains at $x = 0$ and $x = L$ respectively.

The displacement u_L is a measure of mass, so in the following discussion it will sometimes be referred to as the mass it represents rather than displacement.

In the unified model, equation (20) is used as one of three sources of downstream boundary displacement. The other sources are roller motion and initial uniaxial strain.

The continuity equation and boundary condition for the _u_ displacement

In the unified model, roller motion contributes both directly and indirectly to the x-direction displacement, u.
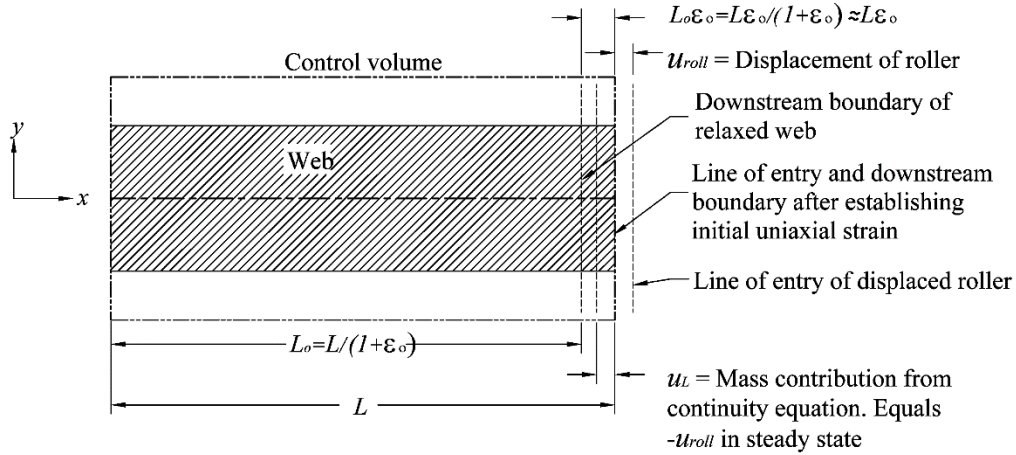

Figure 2
Definitions for control volume

In Figure 2, a simple example of boundary motion is illustrated. The control volume boundaries are indicated by double dash lines. The downstream end of the volume coincides with the line of entry to the roller when the web is in a state of initial uniaxial strain ε_o. To simplify discussion, the simplest possible case is considered where it is assumed that the roller abruptly moves a distance u_{roll} [1] in the x direction while remaining parallel to the upstream roller. The control volume remains fixed at $x = L$. The roller displacement u_{roll} causes the strain in the span to increase and mass in the control volume to decrease. The strain change simultaneously causes the

---

[1] This kind of motion wouldn't occur in practice.

continuity equation to begin restoring the mass that has moved outside the control volume by creating a negative displacement u_L. The magnitude of u_L continues to grow in the negative direction and the mass it contributes to the span increases until it reaches a steady state where it is equal to $-u_{roll}$. At this point, the strain in the span is restored to its original value of ε_o and the net displacement $\varepsilon_o{\cdot}L$.

So, the complete boundary condition for x-direction displacement u at $x = L$ for a roller that is displaced by a distance u_{roll} is,

$$u_{boundary} = u_L + u_{roll} + \varepsilon_o L \tag{21}$$

The continuity equation (22) supplies part of the x-direction boundary condition at $x = L$.

$$\frac{d}{dt}\left(-u_L\right) = V_1\left(1 - \varepsilon_{x0}\right) - V_2\left(1 - \varepsilon_{xL}\right) \tag{22}$$

For a realistic application in which the roller pivots and/or shifts laterally, the quantity u_{roll} becomes a function of pivot angle θ_r, y, time and shift d_{shift} of the pivot point. The lateral displacement v_L accounts for movement of the web relative to the pivot point. So, to model rollers that pivot and shift, uroll can be defined as,

$$u_{roll} = \theta_r\left(y + v_L - z\right)$$
$$\theta_r = \theta_{pivot} f_{ramp} \qquad z = d_{shift} f_{ramp} \tag{23}$$

where, θ_{pivot} is the maximum extent of roller pivot angle, v_L is lateral displacement of the web at $x = L$ and d_{shift} is the maximum extent of the lateral shift of the roller. The function f_{ramp} is an s-shaped ramp function that smoothly transitions from zero to unity in a specified rise time.

Earlier use of the continuity equation in lateral dynamics

Michael Leport, in 1985, set the time derivative of (18) to zero and used it to establish a steady state boundary condition for a concave roller model [7]. The author did the same thing in 2005 [8].

The normal entry equation and boundary condition for the v displacement

When doing two-dimensional elastic analysis of moving webs there is a conceptual problem that doesn't arise when using beam theory. In beam theory there is no confusion about the definition of a quantity like slope, because the model is essentially one-dimensional, and we talk about slope of the centerline or of the neutral axis. But, in a two-dimensional model using elasticity theory, where a quantity like slope must be applied at each point across the width of the web, the definition is less obvious. The quantity that's needed is the instantaneous direction of the transport velocity of the deformed web. This can be found by first defining MD motion trajectories in the relaxed web as straight lines, parallel to the centerline. The slopes of these lines in the deformed web, then become everywhere instantaneously tangent to the velocity field of the web. In fluid dynamics, these would be called streamlines.

The normal entry equation (24) in the context of elasticity theory is,

$$\frac{dv_L}{dt} = V_2\left(\theta_r - \frac{\partial \eta_L}{\partial \xi}\right) + \frac{dz}{dt} \tag{24}$$

where v_{L2} is the lateral displacement at $x = L$, θ_r is the roller angle and $\partial\eta_L/\partial\xi$ is the slope of a tangent to a streamline in the deformed web at $x = L$. Using relations (13),

$$\frac{\partial \eta_L}{\partial \xi} = \left[\frac{\partial v_L}{\partial x}dx + \left(1 + \frac{\partial v_L}{\partial y}\right)dy\right]\left[\left(1 + \frac{\partial u_L}{\partial x}\right)dx + \frac{\partial u_L}{\partial y}dy\right]^{-1} \tag{25}$$

Since the y variation of the streamline of the undeformed web is zero, (25) reduces to,

$$\frac{\partial \eta_L}{\partial \xi} = \frac{\partial v_L}{\partial x}\left(1 + \frac{\partial u_L}{\partial x}\right)^{-1} \tag{26}$$

And (24) becomes,

$$\frac{\partial v_L}{\partial t} = V_2\left[\theta_r - \frac{\partial v_L}{\partial x}\left(1 + \frac{\partial u}{\partial x}\right)^{-1}\right] + \frac{dz}{dt} \tag{27}$$

Equation (27) is one of two parts of the y-direction boundary condition,

$$v_{boundary} = v_L - \mu\varepsilon_o y \tag{28}$$

This is the normal entry equation for the elasticity model. It provides the y-direction boundary condition at $x = L$ and is applied at each point across the width of the web. The roller angle θ_r and z have the same definitions as in equation (23).

Complete model

The equations of equilibrium:

$$\frac{\partial}{\partial x}\left[\sigma_{xx} - \omega_z\tau_{xy}\right] + \frac{\partial}{\partial y}\left[\tau_{xy} - \omega_z\sigma_{yy}\right] = 0 \tag{29}$$

$$\frac{\partial}{\partial y}\left[\sigma_{yy} + \omega_z\tau_{xy}\right] + \frac{\partial}{\partial x}\left[\tau_{xy} + \omega_z\sigma_{xx}\right] = 0 \tag{30}$$

Normal entry equation:

$$\frac{\partial v_L}{\partial t} = V_2\left[\theta_r - \frac{\partial v_L}{\partial x}\left(1 + \frac{\partial u}{\partial x}\right)^{-1}\right] + \frac{dz}{dt} \tag{31}$$

Continuity equation:

$$\frac{\partial}{\partial t}\left(-u_L\right) = V_1\left(1 - \varepsilon_{x0}\right) - V_2\left(1 - \varepsilon_{xL}\right) \tag{32}$$

x-direction boundary condition:

$$u_{boundary} = u_L + u_{roll} + \varepsilon_o L \tag{33}$$

$$u_{roll}(y,t) = \theta_r\left(y + v_L - z\right)$$

$$\theta_r = \theta_{pivot} f_{ramp} \qquad z = d_{shift} f_{ramp} \tag{34}$$

y-direction boundary condition:

$$v_{boundary} = v_L - y\mu\varepsilon_o \tag{35}$$

The last two equations in (34) can be manipulated to create a pivot-only or shift-only roller. They can also be used to create a configuration in which a roller is simultaneously shifted and pivoted to create a "steering" guide. Parameter θ_r is the maximum extent of a roller pivot motion and d_{shift} is the maximum extent of a roller shift. The function f_{ramp} is an s-shaped unit ramp function with adjustable rise and delay times.

Implementation in FlexPDE

FlexPDE is a general purpose partial differential equation solver. It turns a description of a system of partial differential equations (steady state or time dependent) into a finite element model, solves the system, and presents graphical output of the results.

Figure 3 shows a portion of the script used to produce the data for the pivoting roller in the next section[2]. This is for a web that is initially in a state of uniaxial stress between parallel rollers.

---

[2] The complete script is available on request.

At $t = 0$ the downstream roller is pivoted by angle *ang* using a smooth-cornered ramp function called *pos* having a rise time of *0.1* second and an amplitude of *1.0*. The web in the previous span is assumed to be in a state of uniaxial strain, ε_o.

```
theta_r = ang*pos(0.1, 0)
d_shift = 0
z = d_shift*pos(0.1, 0)
dtz = d_shift*vel(0.1, 0)

initial values
U = exo*x
V = -y*exo*nu

equations
U: dx(Sx - wz*Txy) + dy(Txy - wz*Sy) = 0
V: dx(Txy + wz*Sx) + dy(Sy + wz*Txy) = 0
V_b: dt(V_b) = Vo*( theta_r - vx/(1+ex)) + dtz
U_b: dt(-U_b) = Vu/(1+exo) - Vd/(1+ux)

boundaries
 region 1
   start 'perimeter1' (0, W/2) mesh_density = 10
      value(U) = 0
      value(V) = -y*exo*nu
   line to (0, -W/2) mesh_density = 1
      load(U) = 0
      load(V) = 0
   line to (L, -W/2) mesh_density = 30
      value(U) = U_b - theta_r*(y+V-z) + exo*L
      value(V) = V_b - y*exo*nu
   line to (L, W/2) mesh_density = 1
      load(U) = 0
      load(V) = 0
   line to close
```

Figure 3
FlexPDE script showing equations, domain definition
and boundary conditions

The upstream boundary conditions assume uniaxial strain in the previous span. Displacements are fixed at $u = 0$ and $v = -y\varepsilon_o\mu$, where μ is Poisson's ratio. These conditions are specified in the first segment of the "boundaries" section.

Theta_r is defined as the *ang·pos(0.1, 0)*, where *ang* is the maximum extent of the roller pivot and *pos* is a smooth-cornered ramp function with an amplitude of *1* and rise time of *0.1* sec.

d_shift is the maximum extent of shift of the roller pivot point. It is set to zero in this case.

z is *d_shift·pos(0.1, 0)*

There are four relationships in the "equations" section. The first two are the nonlinear equations of equilibrium for small rotations. The second two are the normal entry and continuity equations. Ordinarily the relationships used for boundary conditions are specified in the "boundaries" section. However, since the normal entry and continuity equations define $\partial v/dt$ and $\partial u/dt$, they must be placed in the "equation" section where they will be integrated to make values of *v* and *u* available. These special values of *u* and *v* are given names *U_b* and *V_b* to set them apart from the main problem variables.

In the boundaries section, *U_b* and *V_b* are used in the definition of *u* and *v* at the downstream boundary. The definition of *u* consists of three parts

1. *exo ·L* for the initial uniaxial stress.
2. *-Theta_r(y+V-z)* for the change in roller angle
3. *U_b* for mass change.

The definition of *v* has two parts.

4. *-y·exo·nu* for the Poisson contraction due to the initial uniaxial stress.
5. *V_b* for lateral displacement caused by the roller.

COMPARISON OF THE 2D ELASTICITY MODEL WITH MODELS BASED ON BEAM THEORY

The new model has not been tested experimentally; however, its behavior can be compared to the E-B static and dynamic models tested by Shelton in his dissertation. It can also be compared to a model that is closely related to Shelton's, but includes the effect of shear, (Timoshenko beam model) described in "The Effect of Mass Transfer on Multi-Span Lateral Dynamics of Uniform Webs" [1].

To enable comparison of the one-dimensional and two-dimensional models, the 2D elasticity values have been averaged over the width of the web.

Comparisons with Timoshenko beam model

The time histories in the next four figures compare outputs from the Timoshenko dynamic beam model with the new 2D elasticity model for a roller pivot of 0.001885 radians. The input motion was a ramp function beginning at t = 0 with a rise time of 0.1 second.

The application parameters are the same as Shelton's first set of experimental parameters listed on page 45 of his dissertation [2]. Tension = 36.7 Lbf, Span length = 19.5 inches, Width = 9.03 inches, thickness = 0.009 inch, KL = 0.2364, modulus = 450,000 psi. Line speed was 100 in/sec.
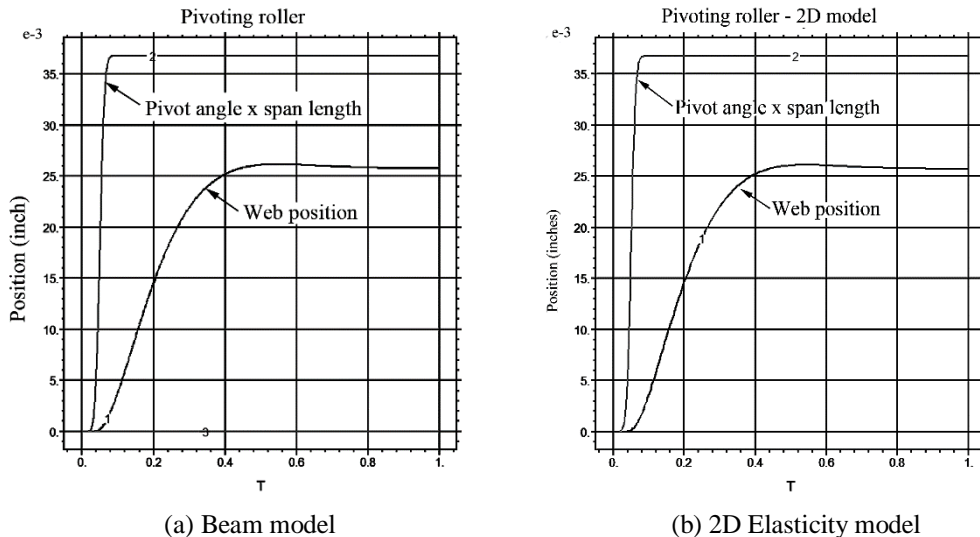

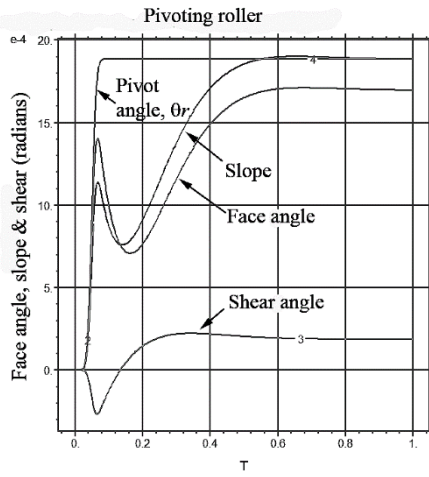(a) Beam model   (b) 2D Elasticity model
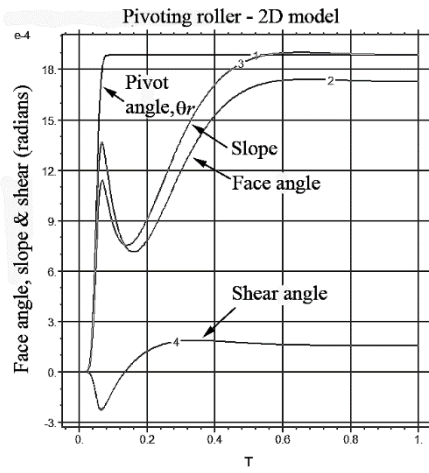
Figure 4
Lateral position, pivoting roller
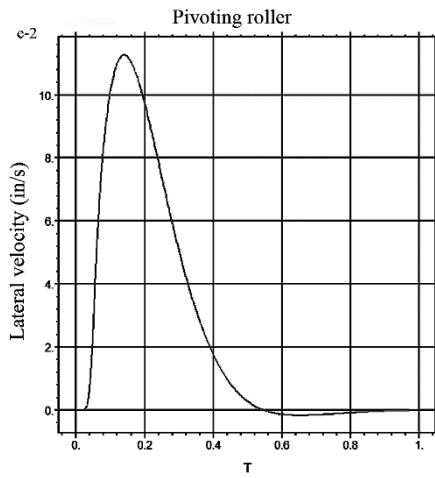
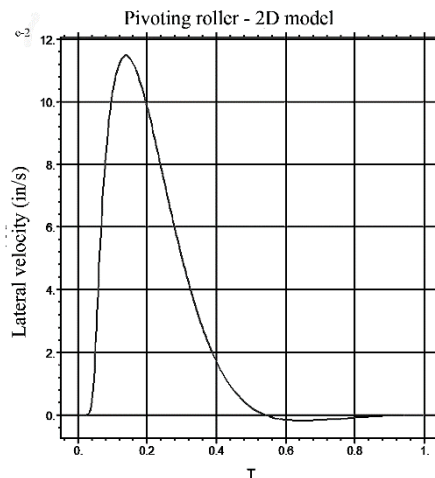(a) Beam model   (b) 2D Elasticity model

Figure 5
Slope, face angle and shear, pivoting roller

(a) Beam model   (b) 2D Elasticity model

Figure 6
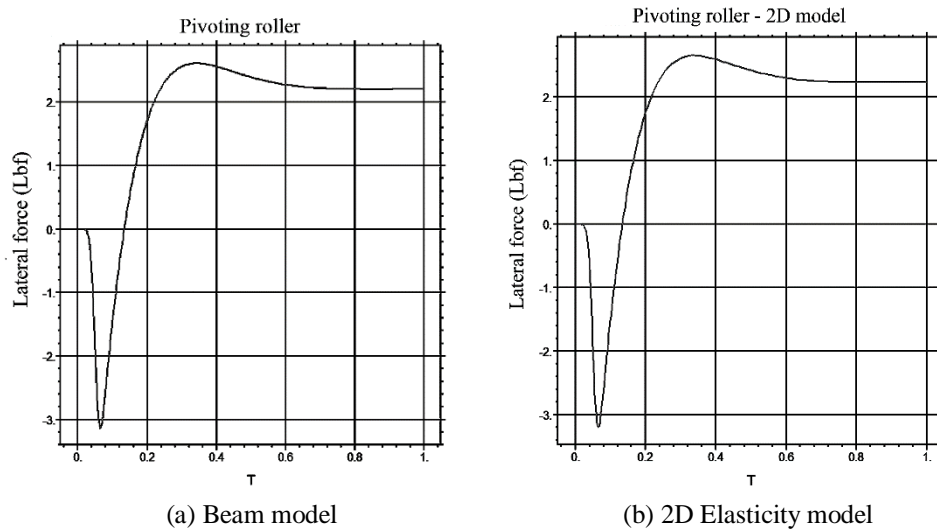Lateral velocity, pivoting roller

(a) Beam model   (b) 2D Elasticity model

Figure 7
Lateral force, pivoting roller

Comparison with Shelton's steady state model

The curves in the graph of Figure 8 show the evolution over time of the elastic curve of the web centerline in the 2D elasticity model. After five time constants, it coincides so closely with Shelton's steady state solution that the two curves are indistinguishable. Application parameters were the same as used for the previous example.
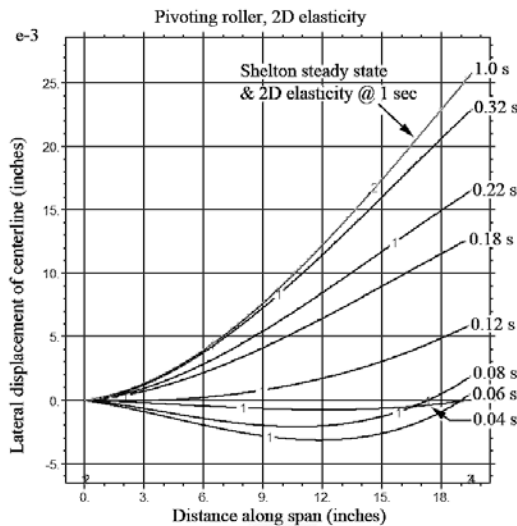

Figure 8
Comparison with Shelton's steady state model
after 5 time constants.

Comparison with Shelton's dynamic model

To verify his E-B dynamic model, Shelton ran four dynamic tests in which he applied a sinusoidal displacement to a downstream roller and measured the lateral displacement of the web. In two of them, a downstream roller was shifted on inclined linear bearings so that it simultaneously pivoted in the plane of the web about an instant center in the entering span (an arrangement commonly used in web guides). The dashed curve in Figure 9 shows the predicted amplitude response for one of them. This same curve is shown in Figure 4.7.7 of his dissertation along with the experimental data points that confirmed its accuracy.

Sinusoidal inputs were applied to the 2D elasticity model at the same frequencies used by Shelton for his tests and allowed to run for five time constants. The resulting amplitude ratios are plotted on the graph as black dots. It is apparent that the two models agree closely.

Parameters for Shelton's test are: Span length = 63 inches, Width = 1.5 inches, Thickness = 0.009 inches, Modulus = 510,000 psi, Tension = 30 Lbf, Speed = 100 inches/sec, Instant center radius = 18.09 inches.
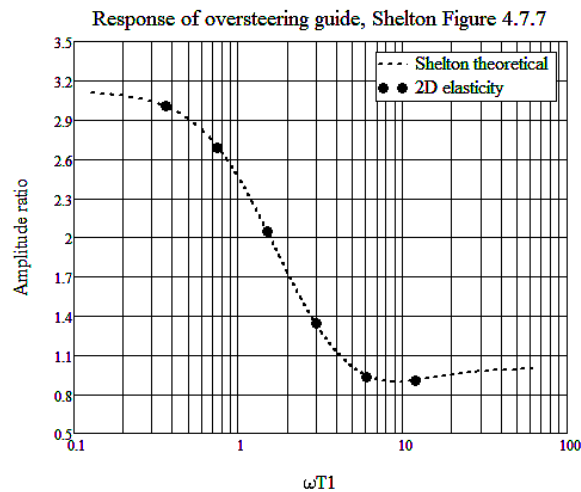

Figure 9
Comparison with Shelton's Dynamic E-B model
for an oversteering guide roller

Comparison with Shelton's steady state test data

Shelton tested his steady state E-B model by measuring lateral force at the downstream roller. Although the main purpose of the measurement was to validate the zero-moment boundary condition, he chose to use lateral force as a proxy because it was believed to be much easier.

Comparison of results for all 21 of Shelton's steady state tests are shown in Figure 11 below. To establish validity of his 4th boundary condition (zero moment at $x = L$) he compared the measured value of lateral force at $x = L$ (column 5) with the value predicted by his model (column 8). The value predicted by the Timoshenko model (based on mass transfer) is shown in column 10. The value predicted by the 2D elasticity model is shown in column 12. The percent errors are calculated as 100(model N_L – experimental N_L)/experimental N_L.

There is no mention of the line speed used for the tests. I assumed 100 in/s.

Values from the Timoshenko and 2D elasticity models were taken after 5 time constants (L/V).

All but three of the force values of the Timoshenko model are slightly lower than those of the corresponding E-B model and the exceptions were equal to rather than less than. This makes sense because shear would reduce the stiffness of the beam. However, when the absolute values of all the errors are compared, neither model seems to have an advantage. This also makes sense because the ratio of length to width of all the test cases was greater than 2, making the effect of shear negligible.

#	Shelton Experimental data							SS E-B beam model		Dynamic Tim. Model		2D elasticity model	
	1	2	3	4	5	6	7	8	9	10	11	12	13
	T (Lbf)	L (inch)	W (inch)	θ_r (rad)	N_L (Lbf)	KL	$N_L/T\theta_L$	N_L (Lbf)	% Diff	N_L (Lbf)	%Diff	N_L (Lbf)	% Diff
1	36.7	19.5	9.03	0.001885	2.375	0.2364	34.3	2.46	3.58	2.21	-6.95	2.24	-5.68
2	36.7	19.5	9.03	0.001885	2.45	0.2364	35.4	2.46	0.41	2.21	-9.80	2.24	-8.57
3	55.1	19.5	9.03	0.001885	2.4	0.2904	23.1	2.45	2.08	2.2	-8.33	2.23	-7.08
4	36.7	40	9.03	0.00377	1.1	0.485	7.95	1.15	4.55	1.12	1.82	1.13	2.73
5	55.1	40	9.03	0.00377	1.075	0.594	5.17	1.14	6.05	1.11	3.26	1.12	4.19
6	18.3	56.5	9.03	0.00377	0.575	0.484	8.34	0.576	0.17	0.568	-1.22	0.573	-0.35
7	55.1	56.5	9.03	0.00377	0.55	0.842	2.644	0.554	0.73	0.547	-0.55	0.552	0.36
8	55.1	63	4.48	0.01884	0.15	2.684	0.1445	0.164	9.33	0.164	9.33	0.165	10.00
9	9.1	40	4.48	0.00377	0.125	0.694	3.64	0.138	10.40	0.137	9.60	0.137	9.60
10	36.7	40	4.48	0.00377	0.125	1.392	0.903	0.122	-2.40	0.122	-2.40	0.123	-1.60
11	36.7	40	4.48	0.00941	0.325	1.392	0.941	0.305	-6.15	0.304	-6.46	0.306	-5.85
12	36.7	20	4.48	0.00377	0.525	0.696	3.79	0.55	4.76	0.537	2.29	0.542	3.24
13	9.1	20	4.48	0.00377	0.55	0.346	16	0.567	3.09	0.553	0.55	0.557	1.27
14	18.3	20	4.48	0.00377	0.575	0.491	8.34	0.561	-2.43	0.547	-4.87	0.552	-4.00
15	27.5	20	4.48	0.00377	0.625	0.601	6.03	0.556	-11.04	0.542	-13.28	0.547	-12.48
16	36.7	20	4.48	0.00377	0.625	0.696	4.51	0.55	-12.00	0.537	-14.08	0.542	-13.28
17	9.1	40	4.48	0.00377	0.125	0.694	3.64	0.138	10.40	0.137	9.60	0.138	10.40
18	36.7	40	4.48	0.00377	0.125	1.392	0.904	0.122	-2.40	0.122	-2.40	0.123	-1.60
19	36.7	40	4.48	0.00941	0.325	1.392	0.941	0.305	-6.15	0.304	-6.46	0.306	-5.85
20	36.7	56.5	4.48	0.01884	0.25	1.967	0.362	0.263	5.20	0.262	4.80	0.264	5.60
21	55.1	56.5	4.48	0.01884	0.2	2.408	0.1925	0.226	13.00	0.227	13.50	0.228	14.00

Figure 10

Comparison of Shelton's E-B model with the Timoshenko and 2D elasticity models

Shelton did not perform tests on any configurations with an *L/W* less than 2.16. To get some idea of what to expect, it is instructive to compare the models for small *L/W*.

Parameters						SS E-B beam model	Dynamic Tim. Model	2D elasticity model
1	2	3	4	5	6	7	8	9
L/W	T (Lbf)	L (inch)	W (inch)	θ_r (rad)	θ_{cr} (rad)	N_L (Lbf)	N_L (Lbf)	N_L (Lbf)
2.16	36.7	19.5	9.03	0.001885	0.00215	2.46	2.21	2.24
1.62	36.7	14.625	9.03	0.0014138	0.00162	3.28	2.74	2.79
1.08	36.7	9.75	9.03	0.0009425	0.00108	4.93	3.41	3.49
0.54	36.7	4.875	9.03	0.0004713	0.000541	9.87	3.54	3.64

Figure 11

Comparison of models for small *L/W*.

In each case the pivot angle was chosen to be slightly less than the value at which a slack edge would begin to develop at the upstream roller.

It is apparent that for values below 2.0, the Timoshenko and elasticity models are in fair agreement, but the E-B model diverges significantly from the other two. Could this mean that the Timoshenko model can be used for small L/W? This is an area that requires future testing.

Dynamic wrinkling

The graph in Figure 12(a) shows the evolution over time of lateral velocity at the downstream roller versus cross-web position following pivoting of a roller. The graph in Figure 12(b) shows the evolution of the principal minimum (lateral) stress over the same period. Application parameters are the same as used for Figure 4 though Figure 7.
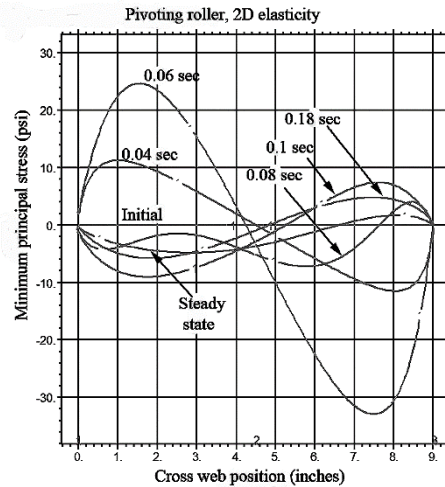
In Figure 12(a) the web is initially in a steady state and the velocity profile is flat, but when it begins moving, lateral velocity is higher at the edges than at the center (cup shaped). At about 0.08 second the center begins to move faster than the edges (cap shaped) and as time increases the velocity profile becomes progressively flatter until it reaches a completely uniform steady state again.

This has implications for wrinkling because the faster portions will advance on the portions ahead of them and create lateral compressive stress.

In Figure 12(b) the principal minimum stress is plotted at several different times. It is this stress, rather than the CD stress that will have the greatest influence on wrinkling. The web starts out in a state of uniaxial stress and the principle minimum stress is zero. Then, as the time progresses a sinusoidal-like stress profile develops with the left side being positive and the right side negative. At 0.06 seconds, a peak negative value of -33 psi is reached. At approximately 0.08 seconds, the profile reverses so that the positive peak is on the right and the negative on the left. This event coincides with a change in shape of the lateral velocity profile. When it reaches steady state, there is a persistent curve in the principal stress profile due to the shear stress necessary to maintain the web deflection.
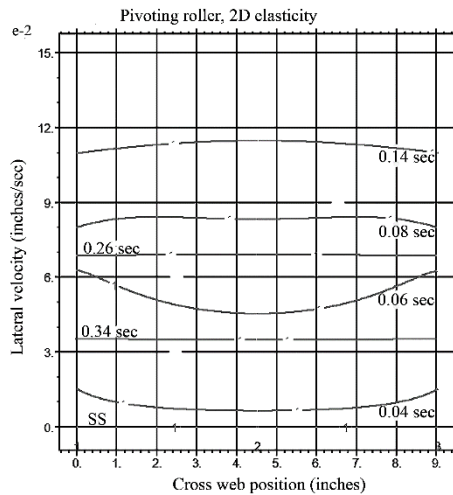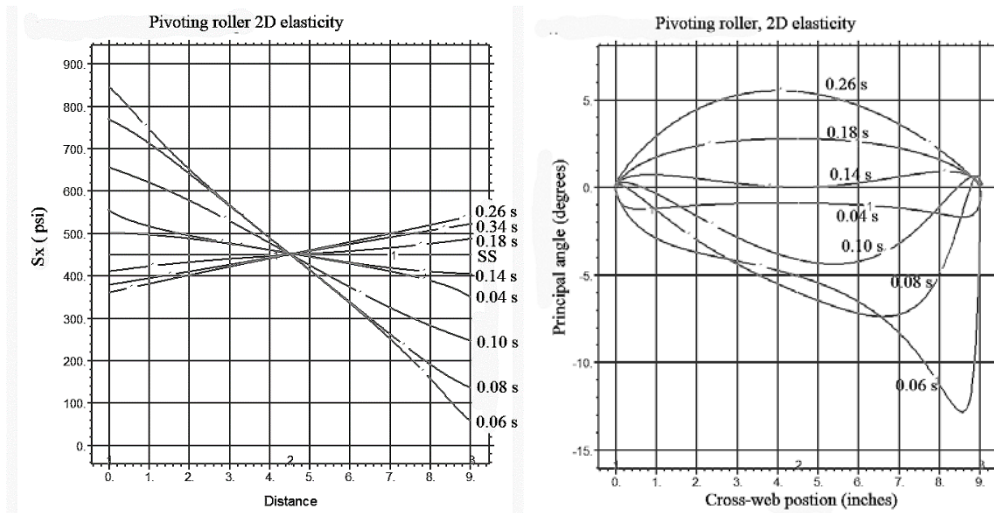

(a) Lateral velocity profile over time   (b) Principle minimum stress over time

Figure 12
Lateral velocity and principal minimum stress at downstream roller
2D elasticity model

(a) MD stress over time   (b) Principal angle over time

Figure 13
MD stress and principal angle at downstream roller
2D elasticity model

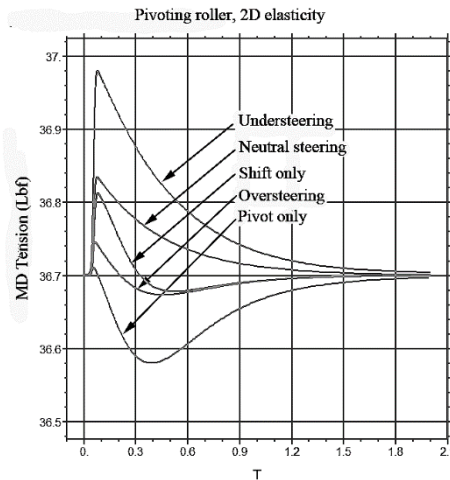## MD tension disturbances due to pivoting and shifting of a roller

Figure 14
Tension disturbances due to roller motion
Ramp functions with 0.1 sec rise time

The curves in Figure 14 show examples of tension disturbance at the downstream roller caused by five different types of roller motion.

Application parameters correspond to Shelton's fourth set of experimental parameters listed on page 45 of his dissertation [2]. Tension = 36.7 Lbf, Span length = 40 inches, Width = 9.03 inches, thickness = 0.009 inch, KL = 0.485, modulus = 450,000 psi.

1. Pivot-only – Pivot angle = 0.00377 radians, lateral shift = 0.
2. Oversteering – Pivot angle = 0.00377 radians, lateral shift = 0.053 inch
3. Shift-only – Pivot angle = 0, lateral shift = 0.105 inch
4. Neutral steering – Pivot angle = 0.00377 radians, lateral shift = 0.105 inch
5. Understeering – Pivot angle = 0.00377 radians, lateral shift = 0.158 inch

Effect of tension change on lateral position

In Figure 15(a), the downstream roller is first pivoted at t = 0 as it was in (a). Then the roller speed of 200 in/sec is decreased by 0.025 percent using a ramp function beginning at t = 2 sec. Another reduction of the same amount is made at t = 4 sec. The span length is 40 inches, so the tension time constant is 0.2 seconds. The disturbance due to pivoting is barely perceptible in (b). The tension starts at 36.5 Lbf and drops to 27.5 Lbf and then 18.4 Lbf due to the speed changes. The lateral position drops only 0.000150 inch at each tension change.

Application parameters were the same as the in the previous example except for an increase in nominal line speed to 200 in/s.

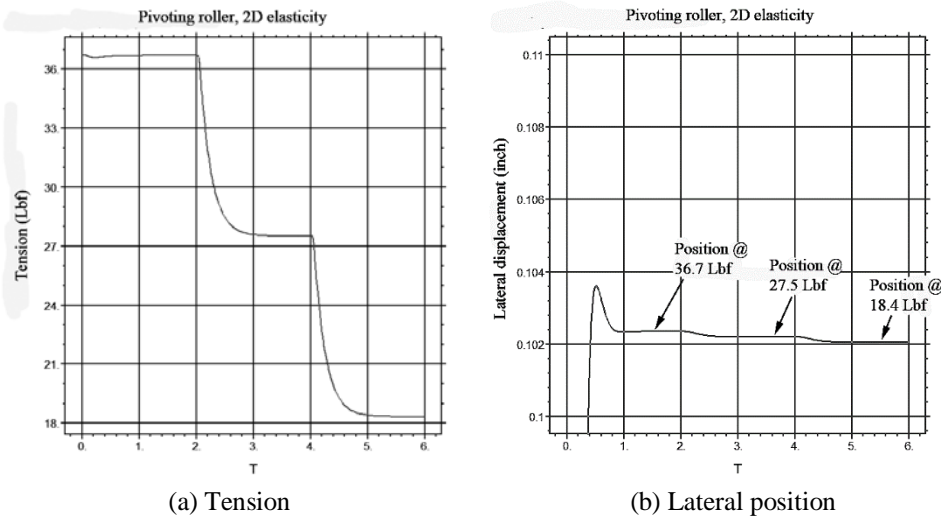The peak in lateral position at 0.5 inch in Figure 15(b) is a transient overshoot from the initial pivot.

(a) Tension   (b) Lateral position

Figure 15
Effect of tension change on lateral position

CONCLUSIONS

The model performed well in the following comparisons.
1. Timoshenko beam model of a pivoted roller
   a. Lateral position
   b. Face angle, Slope and Shear
   c. Lateral velocity
   d. Lateral force
2. Shelton's steady state E-B model - lateral displacement vs distance along span
3. Shelton's dynamic E-B model - frequency response of an oversteering guide
4. Shelton's 21 tests of steady state lateral force

Although new testing should be done, particularly for L/W < 2, the remarkably close agreement with Shelton's static and dynamic test results gives the 2D elasticity model a high degree of credibility and is suggestive of a new conceptual context for further study of lateral web dynamics.

Examples illustrated in this paper were chosen mostly to enable comparison with tested configurations. Implications of the new model, such as tension interaction and dynamic CD behavior, should be explored in areas of application such as,

1. Typical web guide configurations
2. Nonuniform rollers
3. Nonuniform webs

An important limitation of the new model is that it cannot be incorporated directly into control algorithms. Its main utility for control engineers will be its ability to identify and quantify the interaction of lateral and longitudinal systems.

1. Brown, J. L. "The Effect of Mass Transfer on Multi-Span Lateral Dynamics of Uniform Webs", Proceedings of the Fourteenth International Web Handling Conference, June 2017
2. Shelton, J. J., "Lateral Dynamics of a Moving Web", PhD Thesis, Oklahoma State University, July 1968
3. Brown, J. L. "The Connection Between Longitudinal and lateral Web Dynamics" Proceedings of the Fifteenth International Web Handling Conference, June 2019
4. Novoshilov, V. V., "Foundations of the Nonlinear Theory of Elasticity", Graylock Press, 1953
5. Shelton, J. J., "Dynamics of Web Tension Control with Velocity or Torque Control", Proceedings of the American Control Conference, pp 1/5-5/5 1986.
6. Brandenburg, G., "New Mathematical Models for Web Tension and Register Error", Proceedings of the 3rd IFAC Conference on Instrumentation and Automation in the Paper , Rubber and Plastics Industry, vol. 1, 1977
7. Leport, M. L., "The Mechanics of Webs Encountering Concave Rolls", Masters Report, Oklahoma State University, 1985
8. Brown, J. L., "Effects of Concave Rollers, Curved-Axis Rollers and Web Camber on the Deformation and Translation of a Moving Web", Proceedings of the Eighth International Conference on Web Handling, Oklahoma State University, 2005